NUCLEAR STRUCTURE AND NUCLEAR EXCITATIONS FROM ANTIPROTON — NUCLEUS INTERACTION*

J. JASTRZĘBSKI†

CERN, PPE Division, Isolde Group, CH-1211 Geneve 23, Switzerland

P. LUBIŃSKI AND A. TRZCIŃSKA

Heavy Ion Laboratory, Warsaw University
02-097 Warszawa, Poland

for PS203 and PS208 collaboration

(Received December 17, 1994)

The antiproton beam from the Low Energy Antiproton Ring at CERN was recently used in a series of nuclear physics experiments performed by Berlin–Caen–Moscow–Munich–Orsay–Rossendorf–Warsaw collaboration. This paper presents some of the obtained results. In particular a new method of the nuclear periphery study using the annihilation of stopped antiprotons is presented. Also, simple as well as highly exclusive experiments studying the heating of nuclei by antiprotons are discussed.

PACS numbers: 13.75. Cs, 21.10. Gv, 25.43. +t, 36.10. -k

1. Introduction

During last years a number of experiments have been performed in which antiprotons were used to study the nuclear properties. The unique opportunities offered by the Low Energy Antiproton Ring — LEAR at CERN have made these studies possible. The LEAR machine, a part of the CERN Antiproton Accumulator Complex (AAC) was built in early eighties [1–4] giving the first antiproton beam in July 1982. Later, the upgrading of AAC [5] by addition of the Antiproton Collector (ACOL, August 1987) increased its previous beam intensity by a factor of ten. Presently the AAC

* Presented at the XXIX Zakopane School of Physics, Zakopane, Poland, September 5–14, 1994.

† On leave of absence from Heavy Ion Laboratory, Warsaw University

can deliver [6–9] to the experimental areas a pure beam of more than 10^6 antiprotons per second. This beam is characterized by excellent emittance ($\leq 10\pi \times$ mm$\times$ mrad), variable energy (between 2 MeV and 1200 MeV) and a small momentum spread ($\leq 10^{-3}$).

In the present paper we report on some recent applications of the LEAR antiproton beam to the study of nuclear structure and nuclear excitations. There exist a number of earlier reviews, related to the nuclear physics studies with antiprotons [10–16]. We refer to these publications for a wider presentation of the previous achievements in this field.

In Section 2 of this paper we present the new method of the nuclear periphery study which was proposed and realized by the LEAR PS203 experiment during last years. In Section 3, progressing from the simplest to highly exclusive experiments we report on the energy transfer-"heating" of nuclei by pions originating from the annihilation of antiprotons stopped in the medium and captured on Bohr orbits in antiprotonic atoms. Section 4 deals again with the phenomenon of nuclear excitations, this time, however, we discuss the energy transfer from the most energetic antiprotons available using the LEAR facility (PS208 experiment). The article ends by a short summary of the obtained results and the overview of some new experiments, planned for the next years of the LEAR operation.

New method of the nuclear periphery study

2.1. Background

The shape and composition of the nuclear surface has attracted interest almost from the beginning of nuclear physics [17]. The stimulating paper of Johnson and Teller [18] with the suggestion that the nuclear atmosphere is rich in neutrons even for nuclei close to the beta stability line appeared already in 1954 and generated a long going discussion on this subject. Although eventually the main assumption of this work, namely the equality of the proton potential to the algebraic sum of the neutron and Coulomb potentials, was shown to be incorrect, the interest in nuclear surface composition has not ended by this finding. However, at the end of the sixties it became clear that this composition is the effect of a subtle balance between Coulomb and asymmetry effects [19] and can only be guessed from calculations involving a rather high degree of sophistication [20].

Recently, the "neutron skin", often understood as the difference between the rms radii of neutrons and protons, $\Delta R_{\mathrm{np}}^{\mathrm{rms}} = R_{\mathrm{n}}^{\mathrm{rms}} - R_{\mathrm{p}}^{\mathrm{rms}}$, was found to be as large as 0.9 fm in some neutron rich light nuclei [21–26]. This corresponds to about 40% relative difference in these radii. The presently available theoretical and experimental information for heavy nuclei close

to the beta stability line indicates, in spite of their large neutron excess, much smaller values for the neutron skin in these nuclei. For instance, the Hartree–Fock calculations [20] of the charge and neutron rms radii in ^{208}Pb give a neutron skin of a thickness of 0.23 fm or the relative difference between neutron and proton radii, $\Delta R_{\mathrm{np}}/R_0 = 4\%$ (where $R_0 = \frac{1}{2}(R_{\mathrm{n}} + R_{\mathrm{p}})$). The experimental evidence confirms the theoretically calculated values, at least in some cases. Recently, the analysis of the electric giant resonance cross section for α-particle induced excitation [27] gives *e.g.* the $\Delta R_{\mathrm{np}}/R_0$ in ^{48}Ca equal to $(4.1^{+2.1}_{-2.5})\%$ and in ^{208}Pb equal to $(3.0 \pm 1.3)\%$.

Although a rather small value for the neutron skin in heavy nuclei seems to be now well established, this is by no means the whole story of the nuclear surface composition. Already in 1971, *via* the study of sub-Coulomb (p,d) and (d,t) reactions it was shown [28] that at large nuclear distances (significantly above the rms radius) the neutron density of ^{208}Pb exceeds the proton density by orders of magnitude. The study of the interaction of stopped negative kaons [29, 30] and antiprotons [31] with heavy nuclei, clearly a peripheral process, also indicated a high neutron to proton density ratio at large, although not well defined, nuclear distances.

The situation when there is no substantial difference between the first moment (rms radius) of the neutron and proton distribution, but a strong enhancement of the neutron density appears at distances where the matter density is very low, can be called a "neutron halo". Indeed, such a name was already used more than twenty years ago [32] to describe the predominance of neutrons at the nuclear surface. This terminology is adapted throughout this paper.

2.2. Probing the nuclear periphery with antiprotons and kaons

Energetic antiprotons are slowed down in matter by interacting with atomic electrons. When their kinetic energy drops well below one keV they are captured in high-n orbits, forming an "exotic atom". As lower orbits in this antiprotonic atom are empty, the antiproton cascades towards the nuclear surface, first emitting Auger-electrons and later predominantly X-rays. The antiprotonic cascade terminates far above the lowest Bohr orbit, when the antiproton encounters a nucleon on the nuclear surface and annihilates. For nuclei like ^{208}Pb, the lowest accessible antiproton orbits have the principal quantum number $n = 9$ or 10 which corresponds to the orbit radius of $\sim$ 30 fm, much larger than the rms radius of the nuclear matter distribution in this nucleus. The maximum of the annihilation probability is situated at a distance equal to about twice the rms radius. The above scenario, with some changes in orbit number and radius, is also valid for negative kaons. Therefore, if an isospin signature of the annihilation could

be found, negative hadrons could be used to probe the composition of the nuclear periphery.

This idea is more than a quarter of century old. Promoted by Jones [33] and Wilkinson [34] it was first experimentally realised by Davis *et al.* [29] who studied the K^- meson interaction with nuclei in nuclear emulsions. The differences in the characteristics of hyperonic and mesonic reaction products after kaon absorption on a proton or on a neutron were used as the isospin signature of the absorption (due to charge conservation the $\Sigma^+\pi^-$ and $\Sigma^-\pi^+$ reaction products indicate the absorption on a proton, whereas the observation of $\Sigma^-\pi^0$ channel implies K^- absorption by a neutron). The emulsion experiment allowed to classify the observed events in two groups: absorptions on light nuclei, characterized by a significant recoil of the nucleus, and absorptions on heavy nuclei (Ag, Br), accompanied by Auger electron tracks. It was found [30, 35] that the absorption of K^- on a neutron is about 5 times more probable in heavy than in light nuclei. Knowing that the K^- absorption takes place in nuclear periphery and assuming a similar neutron and proton distribution in light nuclei this result would indicate an observation of a neutron halo in heavy nuclei [30]. However, it was later shown [36, 37, 17] that the reported experimental data may also be explained without the assumption of a substantial difference between neutron and proton density at the nuclear periphery.

Besides kaons, antiprotons were also used for the search of a neutron halo in heavy nuclei. In 1973 Bugg *et al.* [31] presented the results of their experiment in which the Brookhaven National Laboratory 30-inch hydrogen bubble chamber was exposed to a beam of slow antiprotons. In this chamber the mesonic prongs from carbon, titanium, tantalum and lead targets were investigated. The physics of the experiment was derived from the fact that $\bar{p}p$ and $\bar{p}n$ annihilations produce events with a net charge of 0 and -1, respectively, and from the assumption that the nuclear capture and annihilation processes occur in the nuclear periphery. The net result was expressed as "halo factor", f (in which corrections for the differences in the $\bar{p}n$ and pp interaction potentials and target N/Z ratios were taken into account). This factor showed a tendency to increase as a function of the target mass. For the Pb target it was equal to 2.3 ± 0.5 to be compared with the value 1.0 for carbon. The authors of Ref. [31] claimed this result to be the evidence of the neutron halo in heavy nuclei. However, the necessity to apply numerous corrections to the experimental data has obscured the transparency of the conclusions. Moreover, their subsequent criticism [38] based on a possible charge exchange process not taken into account in the corrections applied made the question legitimate of whether the neutron halo was really observed in Bugg's experiment.

Recently a new method for the detection of the neutron halo in heavy nuclei using annihilation of stopped antiprotons [39] was proposed and applied. The method uses the identification of nuclear rather than mesonic products of the antiproton-nucleus interaction.

The new method relies on the simple observation that for antiproton annihilations at distant orbits there is a large probability, $P_{\rm miss}$, that all pions created during the annihilation miss the target nucleus (of mass number A_t, proton number Z_t and neutron number N_t). As a result, a cold nucleus with mass number $(A_t - 1)$ is produced. The ratio of nuclei produced with one neutron less than N_t to nuclei with one proton less than Z_t is a function of the neutron to proton density at distances r, where the product of $P_{\rm miss}(r)$ and the antiproton annihilation probability $W(r)$ is sizeable. If $(N_t - 1)$ and $(Z_t - 1)$ products are radioactive their production rate can be easily determined by using gamma-ray spectroscopy methods. This enables one to extract a "halo factor"

$$f_{\rm halo} = \frac{N(\bar{\rm p}{\rm n})}{N(\bar{\rm p}{\rm p})} \frac{{\rm Im}(a_{\rm p})}{{\rm Im}(a_{\rm n})} \frac{Z_t}{N_t},$$

where $a_{\rm p}$ and $a_{\rm n}$ are $\bar{\rm p}$p and $\bar{\rm p}$n scattering lengths, respectively. The value of the ratio ${\rm Im}(a_{\rm p})/{\rm Im}(a_{\rm n})$ is taken from [31]. (It is the ratio of the antiproton annihilation probability on a proton to that on a neutron).

The two observables of interest are the absolute yields of two radioactive products with mass number $(A_t - 1)$ (number of nuclei produced by 1000 $\bar{\rm p}$) and their ratio, eventually transformed into the halo factor. When the halo factor is related to the neutron to proton density ratio, the absolute yield of $(A_t - 1)$ nuclei is a signature of the annihilation site: for the same $W(r)$ a larger yield of $(A_t - 1)$ nuclei indicates more distant annihilations.

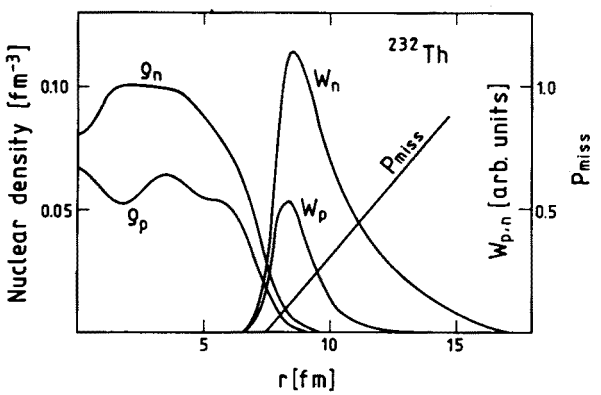

Fig. 1. Neutron and proton densities, $\rho_{\rm n}$ and $\rho_{\rm p}$, the antiproton absorption probability on neutrons, $W_{\rm n}$, and on protons, $W_{\rm p}$, and the "missing probability", $P_{\rm miss}$, for ^{232}Th nucleus. This figure is reproduced from [39].

The calculated neutron and proton densities, the antiproton absorption probabilities and the missing probability are shown in Fig. 1. for the target nucleus ^{232}Th. From this figure it can be estimated that the new method probes the nuclear density at distances around about twice the root mean square radius of this nucleus.

2.3. The recent results

After the publication of the principle of the new method and the first results for ^{232}Th [39] other targets were also investigated using antiprotons from the LEAR facility at CERN. At present the method was applied to nine targets with mass numbers between 58 and 238 [40]. A clear neutron halo effect, correlated with the neutron binding energy, B_n, was observed and is shown in Fig. 2.

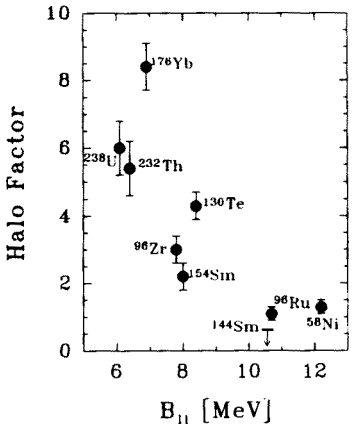

Fig. 2. The recent data of the Warsaw–Munich–Berlin collaboration (PS203 experiment), showing the neutron halo factor (defined in the text) as a function of the target neutron separation energy, B_n. The scattering of the data points indicates that the neutron halo factor depends not only on B_n, but also on some properties of the antiprotonic atom or on the nuclear structure. This figure is adapted from [40].

The significant differences in the halo factor for nuclei with a similar Coulomb barrier (as in ^{96}Ru and ^{96}Zr or ^{144}Sm and ^{154}Sm) demonstrate that we go here beyond a rather trivial effect of the proton wave function attenuation by this barrier. Instead, the correlation of f_{halo} with the neutron separation energy, shown in Fig. 2., classifies the observed effect to the same cathegory of phenomena (although with much smaller magnitude) as the neutron halo effects in light nuclei close to the neutron drip line.

3. Nuclear excitation by stopped antiprotons

After the antiproton annihilation almost 2 GeV energy is released close to the nuclear surface. The questions which can be asked are:

— how much of this energy is transferred to the nucleus ?
— how much of the transferred energy is stored in the nucleus ?
— what is the excitation energy distribution ?
— are there some differences in the decay modes of nuclei, heated without compression and angular momentum transfer in comparison with proton or heavy ion induced reactions ?

In about 95 % of annihilations the 2 GeV annihilation energy is distributed among charged or neutral pion masses and kinetic energies. In remaining cases η or K mesons appear in the final state.

In the antiproton-proton annihilation ("free annihilation", in the absence of a more massive nucleus in the vicinity of the annihilation site) on the average 5 pions are produced from which 3 are charged and 2 are neutral. The pion multiplicity distribution ranges from 2 to 8 pions. Similar numbers are obtained for antiproton-neutron annihilations (see Ref. [12] for more details).

The energy distribution of pions produced after antiproton annihilation extends from zero to about 800 MeV, with the most probable value of about 195 MeV, close to the Δ_{33} resonance in nuclei (*cf.* Fig. 2 in Ref. [12]). Therefore, in case of annihilations on nuclei, pions which enter the nuclear volume are strongly absorbed. In fact, it was shown [15] that for these pions the nucleus behaves as a "black disc" and simple geometrical considerations allow to understand their absorption process, (some numbers are given in the following Section).

Theoretically the energy transfer from the multi-pion system to the nuclear medium is treated by Intranuclear Cascade models (INC). Here again the advent of the LEAR facility clearly boosted the theoretical effort aimed at the prediction and later the explanation of experimental results. The INC models, previously developed for the nucleon-nucleus and pion-nucleus interaction [41–45] are adapted and extended on the antiproton-nucleus physics from the early eighties till now. The groups from Los Alamos [46, 47], Liége [48–52, 16] and Moscow [53–56] are particularly active in this field.

3.1. Mass yield distribution

The simplest experiments giving the information on the excitation energy of nuclei after stopped antiproton annihilations consist of the determination of heavy residual nuclei mass distribution. The so-called radiochemical methods are used here [57, 58]. The shape of the mass yield [59, 60]

and in particular the slope of the yield curve [61, 62] determined for a large mass region can be used to deduce at least relative, if not absolute, excitation energies for a given target. In this way the energy transfer in reactions induced by different projectiles can be compared. Other observables which can be inferred from the mass yield curve and may be used to obtain the information on the excitation energy are the average mass removed from the target nucleus, $\overline{\Delta A}$, and the mass dispersion [63]. The last quantity is equivalent to the slope of the mass yield curve, but has more "objective" character.

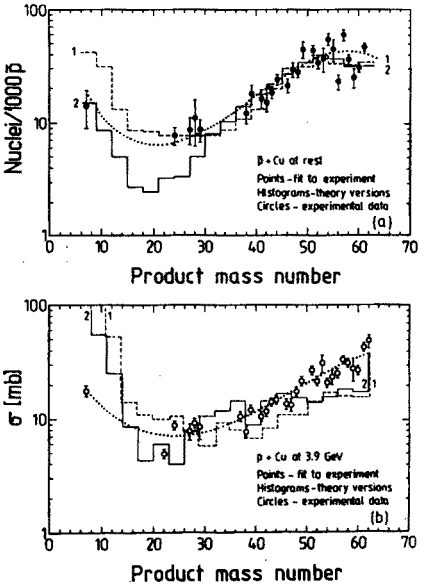

Fig. 3. Mass yields for the production of heavy reaction residues in (a) stopped $\bar{p}+^{nat}Cu$ and $p+^{nat}Cu$ at 3.9 GeV deduced from the experimentally determined cross sections of the radioactive products. The histograms represent two versions of the intranuclear cascade plus evaporation calculation performed by Moscow group [53]. From Ref. [63].

Fig. 3. gives an example of the mass distribution gathered after the stopped antiproton annihilation on ^{nat}Cu target [63]. For comparison the distribution resulting from the 3.9 GeV proton reactions with te same target is also shown. The way of obtaining a relative excitation energy from the mass yield curve is illustrated in Fig. 4. The average removed mass and the mass dispersion values for the antiproton induced reactions on the Cu target are compared there with the corresponding values for reactions induced by protons and pions in a large energy range. From this analysis it was deduced that, on the average, the stopped antiprotons transfer a similar amount of the excitation energy to the ^{nat}Cu target as about 2 GeV protons.

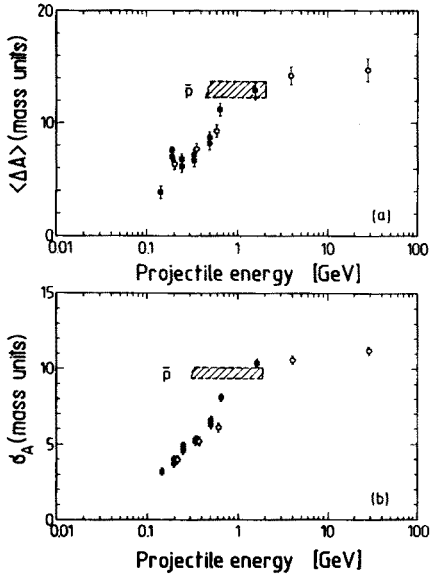

Fig. 4. (a) Average number of removed nucleons, $\langle \Delta A \rangle$, and (b) average dispersion of the mass distribution, σ_A, for pions (solid squares) and protons (open circles) interacting with ^{nat}Cu target. The hatched corridors correspond to (a) $\langle \Delta A \rangle$ and (b) σ_A for stopped antiprotons interacting with ^{nat}Cu target. From Ref. [63].

A similar analysis [64] performed for $\bar{p}$ interacting with Au target indicates that in this case the target excitation energy is more close to the value obtained with 1 GeV protons interacting with gold.

This is illustrated in Fig. 5. where the mass yield obtained after stopped antiproton interaction with Au is compared with a similar distribution observed after 1 GeV proton reactions [65]. Below the product mass of about 187 almost identical mass yields are observed. However, besides previously discussed (see Sect. 3.2.) $(A_t - 1)$ products and perhaps $(A_t - 2)$ ones, heavier masses are clearly depleted for antiprotons. This indicates much narrower energy distribution for stopped antiproton in comparison with proton induced reactions. Indeed, in proton case the masses close to the target originate from the peripheral projectile-nucleus interactions with small energy transfer. In stopped antiproton interactions with nuclei either the annihilation pions miss completely the target nucleus with almost no energy transfer or at least one pion is absorbed. In this case the transferred energy is equal to its rest mass plus kinetic energy, *i.e.* larger than 140 MeV. The observed low yield of close-to-the-target nuclei indicates, that a substantial part of this energy is stored in the nucleus. A similar depletion in the production of nuclei with mass loss below about 10 mass units was also observed for ^{92,95,98}Mo and ^{165}Ho targets [66]. In INC calculation this effect is expected

for two or more pion absorption by the nucleus [53]. However, as discussed in the beginning of Section 4, on the average only about one pion is absorbed after the stopped $\bar{p}$ annihilation on heavy nuclei.

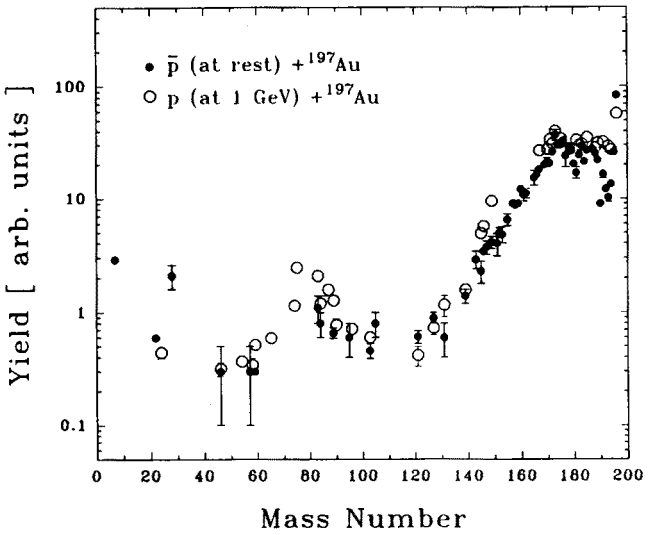

Fig. 5. Mass yields for the production of heavy reaction residues in stopped $\bar{p}$+^{197}Au (solid circles) and p+^{197}Au at 1 GeV (open circles). The antiproton data are from the PS203 experiment and proton from [65]. The antiproton yields were roughly normalized to the proton cross sections in the mass range $170 \leq A \leq 190$.

In Fig. 6. the presently available data on the average removed mass after stopped antiproton interaction with a number of targets are shown. In order to obtain the average excitation energy, $\overline{E^*}$, from the mass yield distribution in absolute units some assumptions (or calculations) should be made or supplementary measurements should be performed. Converting $\overline{\Delta A}$ to $\overline{E^*}$ of the fully thermalised system one should substract from the measured $\overline{\Delta A}$ the average number of nucleons emitted in the fast reaction phase, $\overline{\Delta A}_{\mathbf{fast}}$. Fortunately, the multiplicity of fast non-evaporative nucleons is small [67–70] and the correction for $\overline{\Delta A}_{\mathbf{fast}}$ is of the order of 20%. The remainig value $\overline{\Delta A} - \overline{\Delta A}_{\mathbf{fast}}$ is multiplied by the average energy removed by one evaporated nucleon. Again, this value, often assumed to be about 10 MeV, should be measured [71] or calculated using an evaporation code [72].

The heavy reaction residues produced after stopped $\bar{p}$ interaction with nuclei were observed [66, 73, 63] at masses many tens of mass unit lighter than the target mass. For example masses of A $\approx$ 120 were clearly seen in stopped $\bar{p}$ interaction with ^{197}Au target. This observation indicates that

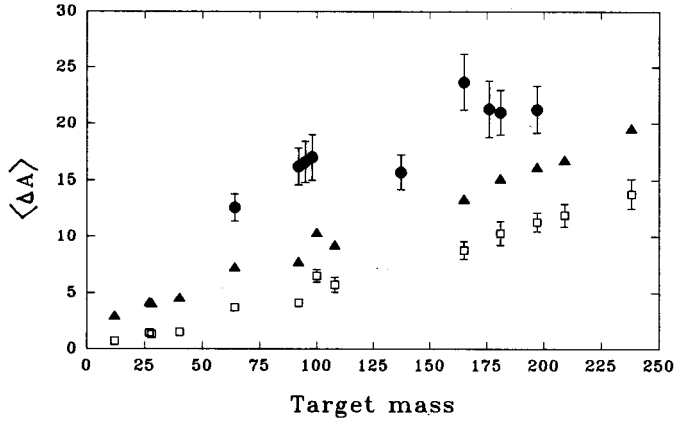

Fig. 6. Comparison of the average number of removed nucleons using various experimental observables. (a) — full circles are $\overline{\Delta A}$ values obtained from the mass yield distribution; (b) — open squares are the average multiplicities of evaporated neutrons; (c) — full triangles represent the sum of (b) and fast neutrons, protons, deuterons and tritons. (See Sect. 3.2. for details). The data are from Refs [66, 73, 63, 70] and PS203 experiment.

the maximal excitation energies obtained with measurable cross sections after stopped $\bar{p}$ interaction with nuclei may reach many hundreds of MeV. However, a precise information on the excitation energy distribution can not be inferred from the mass distribution. It is due to the fact that even for a single excitation energy the observed mass yield would be strongly smeared out by the evaporation process. The distribution of the number of fast, direct or preequilibrium particles should be added to this effect. These facts make any guesses on the excitation energy distribution and its maximum value from the mass distribution hasardous.

3.2. Energetic neutrons and light charged particles

In a recent experiment by Polster and collaborators [74, 70] the thermal excitation energy of a number of targets was determined. A new, elegant and transparent method was used. The light reaction products including neutrons but also $\pi^{\pm}$ and $K^{\pm}$ mesons originating from the antiproton annihilation (but presumably missing the nucleus on which the annihilation took place) were detected using five 10 cm $\times$10 cm ($\phi \times h$) liquid NE213 scintillator detectors. The particle identification was achieved by a simultaneous determination of the pulse shape, time of flight and ΔE energy signal (the last one from a 3 mm thick scintillator placed in front of each NE213 detector). Fig. 7. shows the energy spectra of all identified light particles following the antiproton annihilation at rest on U target. The shape

of the particle spectra for low, undetected energies was obtained assuming maxwellian spectral shape.

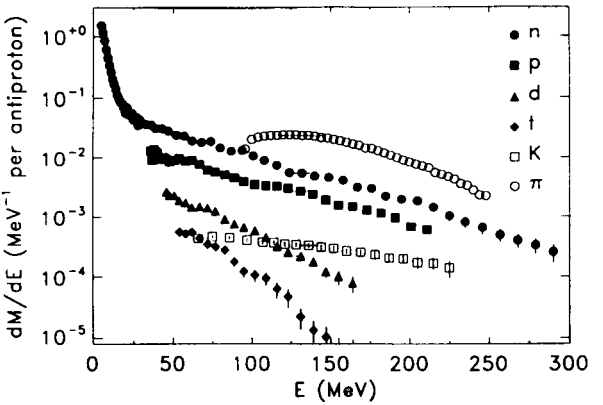

Fig. 7. Energy spectra of all identified particles following antiproton annihilation at rest on uranium target. This figure is reproduced from [70].

The experimental quantities needed for E^* determination are the multiplicities of pions, M_π, and kaons, M_K, the multiplicities of energetic light charged particles, M_{p}, and neutrons, M_{n}, (of energy higher than that of the evaporation particles) and their average energies. Having this a simple arithmetic is played. The average energy transferred to the nucleus from the annihilating antiproton is

$$\overline{E}_{\mathbf{trans}} = 2m_N c^2 - \sum_{i=\pi,K} \langle M_i \rangle [\langle E_{\mathbf{kin}} \rangle + m_i c^2] , \tag{1}$$

where m_N is the nucleon mass and $i = \pi$, K includes also the neutral mesons contribution, assumed to have the same spectral shape as charged mesons.

Before thermalization, fast light particles remove from the nucleus a considerable amount of transferred energy, $\overline{E}_{\mathbf{trans}}$. However, their average multiplicities and average energies are also measured in the same experiment. The energy removal by fast light particles is

$$\overline{E}_{\mathbf{fast}} = \sum_{i=n,p,d,t} \langle M_i \rangle [\langle E_{\mathbf{kin}} \rangle + B_i] , \tag{2}$$

where B_i is particle binding energy. Finally the average excitation energy is

$$\overline{E}^* = \overline{E}_{\mathbf{trans}} - \overline{E}_{\mathbf{fast}} . \tag{3}$$

The determined $\overline{E}_{\mathbf{trans}}$, $\overline{E}_{\mathbf{fast}}$ and $\overline{E}^*$ for investigated targets are shown in Fig. 8. The average excitation energies obtained for $^{\mathrm{nat}}$Cu and ^{197}Au targets from mass yield distributions are also shown in this figure. Although the heavy residue data agree with the light particle ones within errors, slightly lower E^* values seem to be obtained from the mass distribution. This can be at least partly explained by the neglect of fast He emission in the formula (2). The He particles following stopped antiproton absorption [67] were not identified in Polster's experiment.

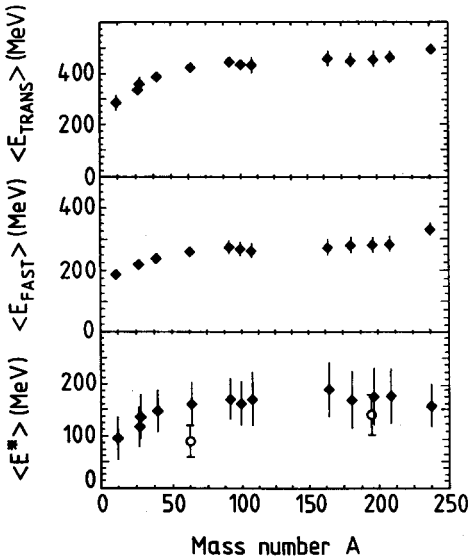

Fig. 8. Target mass dependence of the average energy transferred to the nucleus, $\overline{E}_{\mathrm{trans}}$, (a); of the average energy removed by fast particles, $\overline{E}_{\mathrm{fast}}$, (b); and of the average excitation energy of the thermalized system (c) (adapted from [70]). On the lower panel the data gathered from the mass yield distribution for $^{\mathrm{nat}}$Cu and ^{197}Au targets are also shown (PS203).

3.3. "8π" exclusive experiment

The most reliable method allowing to obtain the excitation energy distribution in nuclei, when the fast reaction phase is terminated, consists in event by event determination of the evaporated neutron multiplicity using 4π neutron detectors [75]. Two such devices are available in Europe: the 1400 l volume Berlin Neutron Ball (BNB) at Hahn–Meitner–Institut and the 3000 l volume ORION detector at GANIL. We refer to [76] for the detailed description of their operation mode and performances. In short these detectors determine the number of slow neutrons accompanying each nuclear

reaction occuring in the target placed in the central part of the detector. This is achieved by counting individual neutron light pulses appearing after the neutron thermalization in the tank filled with the liquid scintillator loaded with gadolinium (large cross section for $(n_{\text{thermal}}, \gamma)$ reaction). The detector efficiency is high for slow, evaporative neutrons ($\approx$ 85% for the spherical shell BNB) and decreases sharply when the neutron energy increases.

In 1994 the BNB detector was mounted in one of the LEAR beam lines. In the inner part of the neutron tank another 4π set-up, the Berlin Silicon Ball (BSIB) consisting of 157, 500 μm thick, Si detectors was placed. These detectors, through charged particle energy, pulse shape and time of flight determination (10 cm flight path) allowed the identification of p, d, α, intermediate mass fragments and fission fragments. The highly segmented structure of BSIB allows also to determine the angular correlations between various charged particles. Fig. 9 shows the schematic view of the two 4π spheres.

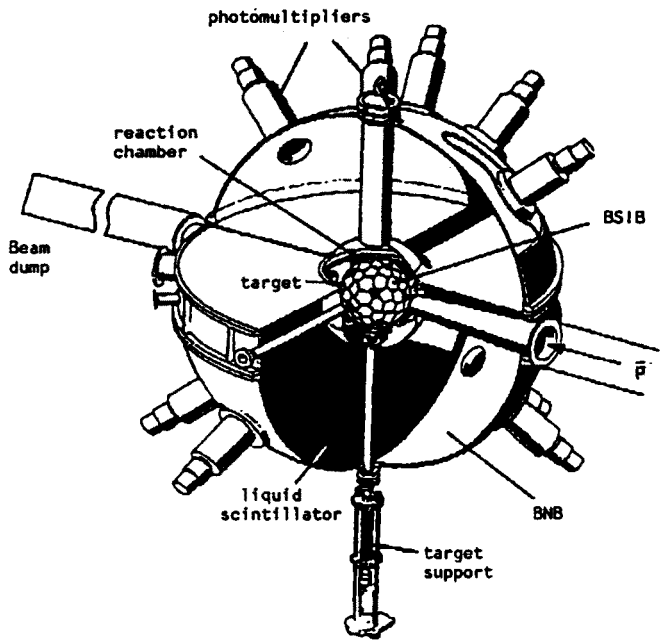

Fig. 9. Schematic drawing of the 4π Berlin Neutron Ball (BNB) and the 4π Berlin Silicon Ball (BSIB) used during recent PS208 experiment. (From [77]).

The antiproton experiments using this set-up were performed quite recently so that at present only very preliminary data, mainly collected online, are available [77]. Fig. 10. shows the measured neutron multiplicity

distribution (not corrected for the detector efficiency) for a series of targets from C up to U. These distributions are quite different than those observed for 0.5 and 2 GeV proton induced reactions [78]. In proton case an enhancement of the low multiplicity events followed by a flat distribution was observed. On the contrary, the neutron multiplicity distributions after stopped antiproton interactions exhibit clear maxima. The measured neutron multiplicity corresponding to these maxima increases with the target Z, being about 15 units for Au target in good agreement with the evaporation neutron data presented in Fig. 6.

The lack of zero neutron multiplicity events is, at first glance, surprising in view of the previously discussed abundant production of the $(A_t - 1)$ nuclei. This can be explained by the "instrumental" effect, characteristic for the study of the antiproton annihilation with large neutron detectors. Besides neutrons, these detectors are also sensitive to pions, accompanying each act of the antiproton annihilation (via the neutron production in the $\pi + C$ reaction on the scintillator compound). In case of the $(A_t - 1)$ isobar production on the average 5 pions are "available" for the interaction with the detector scintillator. These pions shift the zero neutron multiplicity events by a few units leading, for heavy targets, to the low multiplicity local maxima, observed in Fig. 10.

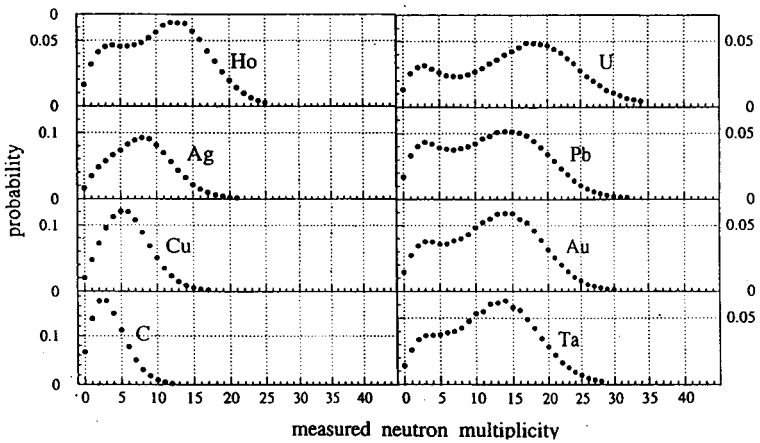

Fig. 10. Measured inclusive neutron multiplicity for stopped antiprotons interacting with various targets. These data are not corrected for the BNB efficiency and pion contribution (from PS208 experiment). The data presented in this figure, together with simultaneously determined charged particle energies and multiplicities will eventually allow to deduce the thermal energy distribution in nuclei after stopped antiproton annihilation.

4. Nuclear excitation by energetic antiprotons

In previous section it was shown that from the tremendous energy available after the stopped antiproton annihilation, only a small part is stored in the interacting nuclei in form of the thermal excitation. There are two effects which contribute to this phenomenon. First, the nucleus itself seems to be unable to distribute fast enough the excitation energy supplied by the absorbed pions on a large number of its constituents. As a result the emission of the fast cascade or preequilibrium particles occurs decreasing substantially the transferred energy (compare Fig. 8.). The second reason is related to a very strong antiproton-nucleon iteraction which makes the antiproton annihilation process in nuclei very peripheral (compare Fig. 1.). This leads to a large number of "escaping" pions, non interacting (or interacting very weakly) with the nucleus on which the annihilation takes place. Indeed, it was shown [52, 70] that even in annihilations on heaviest nuclei on the average only about 20 % of the produced pions is absorbed by the nucleus. As the most probable pion kinetic energy is around 195 MeV (its average kinetic energy is 236 MeV) and its rest mass is 140 MeV, the average transferred energy of about 380 MeV is expected for heavy nuclei. (About 70 MeV higher transferred energy shown in Fig. 8. can indicate some small inconsistencies in the data evaluation of Ref. [70].)

Already many years ago it was advocated [79, 80] that the energetic antiprotons can transfer to nuclei such an amount of the excitation energy that such exotic phenomena as *e.g.* the formation of the quark-gluon plasma can become possible. Although the exotics still remain to be found (perhaps through a careful evaluation of the PS208 data), the arguments for the very large excitation energies transferred to the nuclei from the energetic antiprotons are evidently valid.

With the increase of the antiproton energy the annihilation cross section decreases, making the mean free path of antiprotons in nuclear matter larger. For antiproton momenta larger than 1 GeV/c this mean free path is of the order of one nucleon diameter ($\sim$ 1 fm). Therefore the energy deposition after the annihilation takes place more inside the nucleus and the solid angle under which the annihilation pions "see" the nucleus increases substantially. As the antiproton absorption by nuclear matter is governed by an exponential law, one can expect that for small impact parameters some annihilations will occur in the center of nuclei. After these "central" annihilations a substantial part of created pions will have the energy close to the Δ_{33} resonance in nuclei and will be strongly absorbed by nuclear matter. Such a conversion of a large fraction of the annihilation energy into the kinetic energy of nucleons can be expected for 0.5 $\div$1% of all events in $A \approx 50$ nuclei [48, 46].

Besides events with extremely large energy deposition, the average transferred energy should also increase for energetic antiprotons. To the above mentioned arguments of the less pheripheral annihilation site, the kinematical focusing of the created pions should be added. This focusing will additionally increase the nuclear solid angle seen by the annihilation pions.

One effect will, however, play in the opposite direction when the antiproton kinetic energy is too high. As it was already indicated above, for the efficient energy transfer the kinetic energy of pions should not be too different than the energy of Δ_{33} resonance in nuclei, and the pion kinetic energy is evidently related to the kinetic energy of the incoming antiproton.

The systematics presented in [52] indicates that for the antiproton kinetic energy of 180 MeV the fraction of absorbed pions by heavy nuclei increases from 20 % (stopped antiprotons) up to 43 %. The cascade calculations from [49] indicate that for this energy the antiproton impinging centrally on $A \approx 100$ target annihilates about 2 fm deeper inside the nucleus and its deposited energy distribution changes drastically. This is illustrated in Fig. 11.

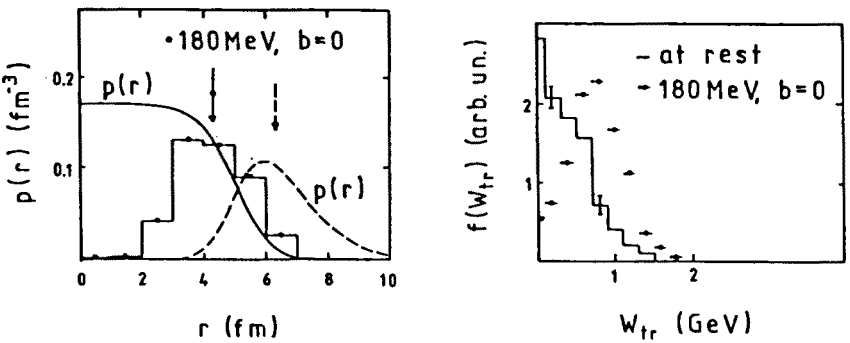

Fig. 11. Left part: distribution of the annihilation sites for stopped (dashed curve) and centrally impinging 180 MeV (histogram) antiprotons interacting with ^{98}Mo target. Right part: distribution of the energy deposit for $\bar{p}$-annihilation at rest and in flight on ^{98}Mo nuclei. This figure is adapted from [49]. See also [46].

During the recent data taking by the PS208 experiment the 585 MeV and 1220 MeV antiproton interaction with a series of target was investigated. The 8π, two spheres detector was again extensively used. Also the mass distributions of heavy reaction residues for ^{nat}Cu, ^{nat}Ag and ^{197}Au targets were studied using radiochemical method.

Fig. 12. shows the preliminary mass distribution for ^{197}Au target bombarded with 1.2 GeV antiprotons. In comparison with stopped antiprotons, the average removed mass $\langle \Delta A \rangle$, is about 20 mass units larger in case of 1.2

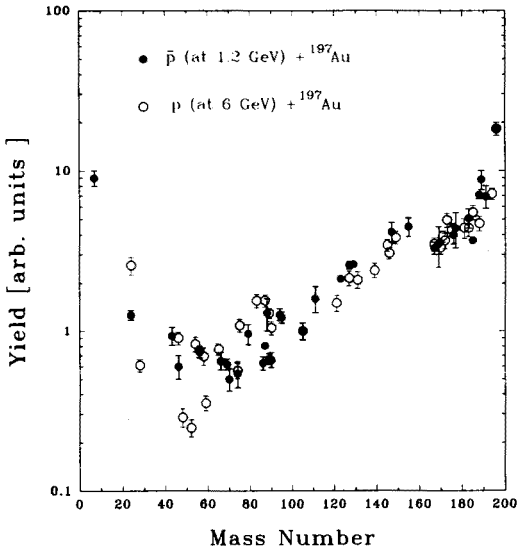

Fig. 12. Mass yields for the production of heavy residues in 1.2 GeV $\bar{p}$+^{197}Au (solid circles) and 6 GeV p+^{197}Au (open circles) induced reactions. The antiproton data are from the PS208 experiment and proton data from [65]. The antiproton yields (as yet available only in arbitrary units) were roughly normalized to the proton cross sections in the mass range $170 \leq A \leq 190$.

GeV antiprotons. In Fig. 12. the mass yield data previously reported [65] for 6 GeV proton induced reactions are also shown. Very similar mass yields are observed indicating a similar average excitation energy reached in both cases. As for higher proton incident energies the shape of the mass yield curve remains almost unchanged [81] the most probably one observes here the highest average energies, which can be accomodated by the gold-like reaction residues. Indeed, as it was already mentioned, the further increase of the antiproton energy would probably drive the pion energy out of the Δ_{33} resonance and, subsequently, decrease the average excitation energy.

The mass yield data allow the comparison of the average excitation energy in *e.g.* proton and antiproton induced reactions. These data are, however, insufficient to give information on events belonging to the extreme tails of the energy distribution for which the most interesting phenomena can perhaps be expected. The two spheres "8π" experiment working on event by event basis constitutes evidently much more powerful approach to the study of these phenomena. This is illustrated in Fig. 13., where the correlation between neutron multiplicity, M_{n}, and charged particle multiplicity, M_{cp}, are displayed for Cu and Au targets. It can be seen that in Cu case at the extreme tails of the multiplicity distributions events with $M_{\mathrm{n}} \approx 20$ and $M_{\mathrm{cp}} \approx 18$ are observed.

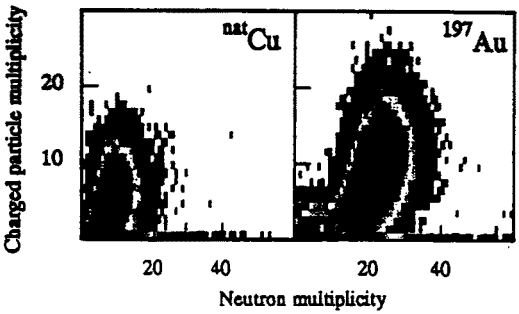

Fig. 13. Correlation of measured charged particle multiplicity, M_{cp}, and neutron multiplicity, M_n, for 1.2 GeV antiproton induced reactions on ^{nat}Cu and ^{197}Au targets. (From [77] and PS 208 experiment).

Taking into account the fact that in charged particle spectra not only protons but also d, t, ^{4}He and heavier intermediate mass fragments are included, this figure shows that in some cases one observes a total desintegration of the Cu target. Further data evaluation, including the angular correlations between charged particles will probably allow the distinction between simultaneous or sequential multifragmentation of this target by 1.2 GeV antiprotons [82].

In Fig. 14. the neutron multiplicities for a serie of targets are shown for $\bar{p}$ kinetic energy of 1.2 GeV. Fig. 15. compares these multiplicities for ^{nat}Cu and ^{197}Au targets at three antiproton energies.

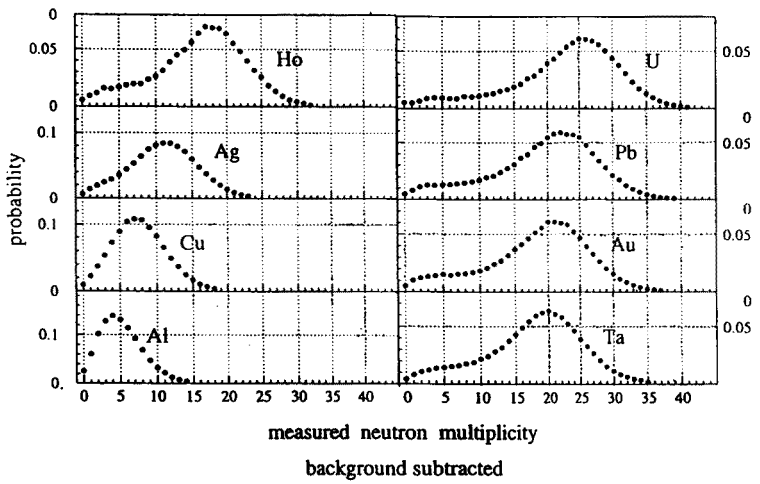

Fig. 14. Measured inclusive neutron multiplicity for 1.2 GeV antiprotons interacting with various targets. These data are not corrected for the BNB efficiency and pion contribution (from PS208 experiment).

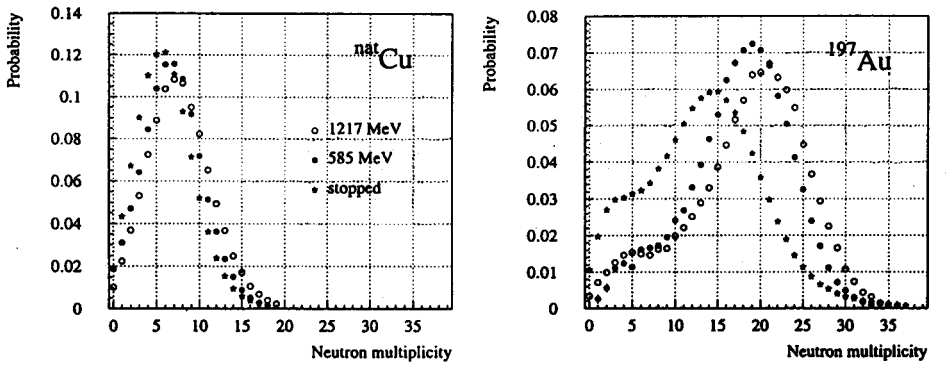

Fig. 15. Comparison of the inclusive neutron multiplicities at three bombarding energies for ^{nat}Cu and ^{197}Au targets: stopped antiprotons — solid squares; 585 MeV bombarding energy — open circles; 1.2 GeV bombarding energy — solid circles. From [77] and PS208 experiment.

These data show that for the heaviest targets the most probable neutron multiplicity increases by about 8 units (the average M_n — slighty more) when the antiproton energy is rised from zero up to 1.2 GeV kinetic energy. Adding to this value the charged particle multiplicity and fast neutrons (detected with much lower efficiency by BNB) one will probably arrive to an agreement with the mass yields data, where the increase of $\langle \Delta A \rangle$ by about 20 mass units was observed between stopped and 1.2 GeV $\bar{p}$ data for Au target. Therefore one deduces that on the average no more than about 20% of the antiproton kinetic energy is added to the annihilation energy in excitation of heavy targets (assuming that removal of one mass unit decreases the excitation energy by 10 MeV).

The nonlinear increase of the neutron multiplicity with the antiproton kinetic energy illustrated for ^{197}Au target in Fig. 15. is the most probably related to the less effective energy transfer for pions with energies much above the Δ_{33} resonance, as previously mentioned.

5. Summary and prospects

In this paper we have briefly described some results gathered recently within PS203 and PS208 experiments performed using LEAR facility at CERN. The very peripheral character of the antiproton annihilation on nuclei was used to test the composition of the nuclear surface. Detecting nuclear annihilation products and determining the production yield of A_{target}-1 nuclei it was shown that the surface of some nuclei is rich in neutrons.

The heating of nuclei with stopped and energetic antiprotons was investigated by various methods going from simple radiochemical studies of the mass yield distribution, through a few counters experiment in which the energy spectra of light charged particle, neutron and meson were measured up to the very sophisticated and highly exclusive experiments using two 4π neutron and charged particle detectors.

A substantial part of these exclusive data still awaits evaluation. What was shown in this paper was mainly based on the on-line glance on small part of collected events. At present it seems already evident, however, that on the average even the energetic antiprotons does not transfer to the nuclei more excitation energy than the energetic protons can do. Some exotic phenomena as complete nuclear desintegrations, occuring with a small cross section can be detected during subsequent data evaluation. For some time, however, a question may remain whether the observation of these phenomena is due to the particularities of the antimatter projectile or rather to a highly exclusive detection method, not previously employed in the study of hot nuclei.

The study of the energy transfer by antiprotons will continue next years. What is missing in the presently collected data are the energy spectra of energetic light particles (including neutrons and mesons) after the 1.2 GeV $\overline{p}$ interaction with nuclei. An experiment similar to the one described in Ref. [69] would provide this information. The repetition of the "8π" experiment with much larger statistics could be also worthwhile, but this will depend on the results of the evaluation of presently available data.

The investigation of the properties of nuclear surface will be continued within recently accepted new experiment PS209. In this experiment the antiprotonic X-rays of nuclei in which neutron halo effects were previously studied will be measured. It is expected that as a result of this experiment new observables, depending on the structure of the nuclear surface but also on the antiproton-nucleus optical potential will be determined. This will substantially constraint the theoretical analysis of the neutron halo effects in heavy nuclei.

The collection of experimental results presented in this paper and their theoretical interpretation was achieved thanks to the effort of many participants involved in our collaboration: W. Bohne, J. Eades, T. von Egidy, P. Figuera, H. Fuchs, J. Galin, F. Goldenbaum, Ye.S. Golubeva, A. Grochulska, K. Gulda, F.J. Hartmann, D. Hilscher, A.S. Iljinov, D.I. Ivanov, U. Jahnke, W. Kurcewicz, B. Lott, M. Morjean, V.G. Nedorezov, S. Neumaier, G. Pausch, A. Peghaire, L. Pieńkowski, S. Proschitzki, I.A. Pshenichov, B. Quednau, S. Schmid, W. Schmid, J. Skalski, R. Smolańczuk, A. Stolarz, A.S. Sudov, S. Wycech. We express our grati-

tude to all of them. In addition we warmly thank Prof. Till von Egidy who introduced our Warsaw team to the experimental nuclear physics with the antiproton beam. The discussions with M. Chanel concerning the Antiproton Accumulator Complex are very appreciated. This work was supported by Grant No 2 P302 010 07 from Polish State Committee for Scientific Research.

REFERENCES

[1] U. Gastaldi, K. Kilian, D. Möhl, in Proc. of 10th Int. Conf. on High-Energy Accelerators, Protvino (1977).
[2] U. Gastaldi, K. Kilian, G. Plass, Rep. CERN/PSCC/79-17 (1979).
[3] P. Lefévre in: Rep. CERN/PS/DL 80-7 (1980).
[4] P. Lefévre in: Physics at LEAR with low-energy antiprotons; Proc. of 4th LEAR Workshop (Villars-sur-Ollon, 1987) p.19, Amsler *et al.* Editors, Harvard Academic Publishers.
[5] E. Jones, in: Physics at LEAR with low-energy antiprotons; Proc. of 4th LEAR Workshop (Villars-sur-Ollon, 1987) p.7, Amsler et al. Editors, Harvard Academic Publishers.
[6] M. Chanel, First Biennial Conference on Low Energy Antiproton Physics, Stockholm, 2-6 July 1990, P. Carlson *et al.* Editors, World Scientific.
[7] S. Baird, J. Bosser, M. Chanel, P. Lefévre, R. Ley, D. Manglunki, D. Möhl, G. Tranquille, *Nucl. Phys.* **A558**, 635 (1993).
[8] M. Chanel, *Nucl. Phys.* **A558**, 467c (1993).
[9] M. Chanel, Rep. CERN/PS 94-38 (AR) (1994).
[10] T. von Egidy, *Nature* **328**, 773 (1987).
[11] C. Guaraldo, *Nuovo Cimento* **102**, 1137 (1989).
[12] J. Cugnon, J. Vandermeulen, *Ann. Phys.* (Paris) **14**, 49 (1989).
[13] H. Machner, Proceedings from DAE Symposium on Nuclear Physics; KFA-IKP(I)-1993-4.
[14] A. Bressani, *Nucl. Phys.* **A558**, 415c (1993).
[15] D. Polster, D. Hilscher, *Phys. Atom. Nucl.* **57**, 1628 (1994).
[16] J. Cugnon, *Phys. Atom. Nucl.* **57**, 1635 (1994).
[17] C.J. Batty, E. Friedman, H.J. Gils and H. Rebel, *Adv. Nucl. Phys.* **19**, 1 (1989).
[18] M.H. Johnson, E. Teller, *Phys. Rev.* **93**, 357 (1954).
[19] D.F. Jackson, *Rep. Prog. Phys.* **37**, 55 (1974).
[20] J.W. Negele, *Phys. Rev.* **C1**, 1260 (1970).
[21] I. Tanihata, H. Hamagaki, O. Hashimoto, S. Nagamiya, Y. Shida, N. Yoshikawa, O. Yamakawa, K. Sugimoto, T. Kobayashi, D.E. Greiner, N. Takahashi, Y. Nojiri, *Phys. Lett.* **B160**, 380 (1985). [22] I. Tanihata, H. Hamagaki, O. Hashimoto, Y. Shida, N. Yoshikawa, K. Sugimoto, O. Yamakawa, T. Kobayashi, N. Takahashi, *Phys. Rev. Lett.* **55**, 2676 (1985).
[23] P.G. Hansen, B. Jonson, *Europhys. Lett.* **4**, 409 (1987).
[24] P.G. Hansen, *Nucl. Phys. News* **1**, 21 (1991).

[25] I. Tanihata, D. Hirata, T. Kobayashi, S. Shimoura, K. Sugimoto, and H. Toki, *Phys. Lett.* **B289**, 261 (1992).
[26] B. Jonson, in Proceedings of the 5th International Conference on Nucleus-Nucleus Collisions, Taormina, 1994, *Nucl. Phys.* **A**, in press.
[27] A. Krasznahorkay, J. Bacelar, J.A. Bordewijk, S. Brandenburg, A. Buda, G. van 't Hof, M.A. Hofstee, S. Kato, T.D. Poelhekken, S.Y. van der Werf, A. van der Woude, M.N. Harakeh, N. Kalantar-Nayestanaki, *Phys. Rev. Lett.* **66**, 1287 (1991). [28] H.J. Körner, J.P. Schiffer, *Phys. Rev. Lett.* **27**, 1457 (1971).
[29] D.H. Davis, S.P. Lovell, M. Csejthey-Barth, J. Sacton, G. Schorochoff, M. O'Reilly, *Nucl. Phys.* **B1**, 434 (1967).
[30] E.H.S. Burhop, *Nucl. Phys.* **B1**, 438 (1967).
[31] W.M. Bugg, G.T. Condo, E.L. Hart, H.O. Cohn, R.D. McCulloch, *Phys. Rev. Lett.* **31**, 475 (1973).
[32] J.A. Nolen, Jr. and J.P. Schiffer, *Annu. Rev. Nucl. Sci.* **19**, 471 (1969).
[33] P.B. Jones, *Phil. Mag.* **3**, 33 (1958).
[34] D.H. Wilkinson, *Phil. Mag.* **4**, 215 (1959).
[35] E.H.S. Burhop, *Nucl. Phys.* **B44**, 445 (1972).
[36] K. Aslam, J.R. Rook, *Nucl. Phys.* **B20**, 397 (1970).
[37] S. Wycech, *Nucl. Phys.* **B28**, 541 (1971).
[38] W.J. Gerace, M.M. Sternheim, J.F. Walker, *Phys. Rev. Lett.* **33**, 508 (1974).
[39] J. Jastrzębski, H. Daniel, T.von Egidy, A. Grabowska, Y.S. Kim, W. Kurcewicz, P. Lubiński, G. Riepe, W. Schmid, A. Stolarz, S. Wycech, *Nucl. Phys.* **A558**, 405c (1993).
[40] P. Lubiński, J. Jastrzębski, A. Grochulska, A. Stolarz, A. Trzcińska, W. Kurcewicz, F.J. Hartmann, W. Schmid, T. von Egidy, J. Skalski, R. Smolańczuk, S. Wycech, D. Hilscher, D. Polster, H. Rossner, *Phys. Rev. Lett.* **73**, 3199 (1994).
[41] V.S. Barashenkov, V.M. Maltser, V.D. Toneev, *Izv. Akad. Nauk SSSR, Ser. Fiz.* **30**, 322 (1966).
[42] K. Chen, Z. Fraenkel, G. Friedlander, J.R. Grover, J.M. Miller, Y. Schimamoto, *Phys. Rev.* **166**, 949 (1968).
[43] G.D. Harp, H. Chen, G. Friedlander, J.R. Grover, J.M. Miller, *Phys. Rev.* **C8**, 581 (1973).
[44] J.N. Ginocchio, *Phys. Rev.* **C17**, 195 (1978).
[45] V.S. Barashenkov, A.S. Iljinov, V.D. Toneev, *Sov. J. Nucl. Phys.* **13**, 743 (1971).
[46] M.R. Clover, R.M. DcVries, N.J. DiGiacomo, Y.Yariv, *Phys. Rev.* **C26**, 2138 (1982).
[47] P.L. McGaughey, M.R. Clover, N.J. DiGiacomo, *Phys. Lett.* **B166**, 264 (1986).
[48] M. Cahay, J. Cugnon, J. Vandermeulen, *Nucl. Phys.* **A393**, 237 (1983).
[49] J. Cugnon, J. Vandermeulen, *Nucl. Phys.* **A445**, 717 (1985).
[50] J. Cugnon, P. Jasselette, J. Vandermeulen, *Nucl. Phys.* **A47**, 558 (1987).
[51] P. Jasselette, J. Cugnon, J. Vandermeulen, *Nucl. Phys.* **A484**, 542 (1988).
[52] J. Cugnon, P. Deneye, J. Vandermeulen, *Nucl. Phys.* **A500**, 701 (1989).
[53] A.S. Iljinov, V.I. Nazaruk, S.E. Chigrinov, *Nucl. Phys.* **A382**, 378 (1982).

[54] Ye.S. Golubeva, A.S. Iljinov, A.S. Botvina, W.M. Sobolevsky, *Nucl. Phys.* **A483**, 539 (1988).
[55] A.S. Botvina, Ye.S. Golubeva, A.S. Iljinov, I.A. Pshenichnov, Preprint INR-742/91.
[56] Ye.S. Golubeva, A.S. Iljinov, B.V. Krippa, I.A. Pshenichnov, *Nucl. Phys.* **A537**, 393 (1992).
[57] G. Rudstam, *Z. Naturforsch.* **A21**, 1027 (1966).
[58] J.B. Cumming, P.E. Haustein, T.J. Ruth, G.J. Virtes, *Phys. Rev.* **C17**, 1632 (1978). [59] D. Gross, L. Satpathy, M. Ta-chung, M. Satpathy, *Z. Phys.* **A309**, 41 (1982).
[60] D.H.E. Gross, *Rep. Prog. Phys.* **3**, 605 (1990).
[61] J.B. Cumming, P.E. Haustein, R.W. Stoenner, L. Mausner, R.A. Naumann, *Phys. Rev.* **C10**, 739 (1974).
[62] J.B. Cumming, P.E. Haustein, H.C. Hseuh, *Phys. Rev.* **C24**, 2162 (1981).
[63] J. Jastrzębski, W. Kurcewicz, P. Lubiński, A. Grabowska, A. Stolarz, H. Daniel, T. von Egidy, F.J. Hartmann, P. Hofmann, Y.S. Kim, A.S. Botvina, Ye.S. Golubeva, A.S. Iljinov, G. Riepe, H.S. Plendl, *Phys. Rev.* **C47**, 216 (1993).
[64] A. Grochulska *et al.*, Warsaw - Münich col.; to be published.
[65] S.B. Kaufman, E.P. Steinberg, *Phys. Rev.* bf C22, 167 (1980).
[66] E.F. Moser H. Daniel, T.von Egidy, F.J. Hartmann, W. Kanert, G. Schmidt, Ye.S. Golubeva, A.S. Iljinov, M. Nicholas, J.J. Reidy, *Z. Phys.* **A333**, 89 (1989).
[67] W. Markiel, H. Daniel, T. von Egidy, F.J. Hartmann, P. Hofmann, W. Kanert, H.S. Plendl, K. Ziock, R. Marshall, H. Machner, G. Riepe, J.J. Reidy, *Nucl. Phys.* **A485**, 445 (1988).
[68] P. Hofmann, F.J. Hartmann, H. Daniel, T. von Egidy, W. Kanert, W. Markiel, H.S. Plendl, H. Machner, G. Riepe, D. Prostic, K. Ziock, R. Marshall, J.J. Reidy, *Nucl. Phys.* **A512**, 669 (1990).
[69] A.S. Sudov, A.S. Botvina, A.S. Iljinov, Ye.S. Golubeva, V.G. Nedorezov, H. Daniel, T. von Egidy, F.J. Hartmann, P. Hofmann, W. Kanert, H.S. Plendl, G. Schmidt, C.A. Schug, G. Riepe, *Nucl. Phys.* **A554**, 223 (1993). [70] D. Polster, D. Hilscher, H. Rossner, T. von Egidy, F.J. Hartmann, J. Hoffmann, W. Schmid, I.A. Pshenichnov, A.S. Iljinov, Ye.S. Golubeva, H. Machner, H.S. Plendl, A. Grabowska, J. Jastrzębski, W. Kurcewicz, P. Lubiński, J. Eades, S. Neumaier, *Phys. Rev.* **C** in print.
[71] W. Skulski, B. Fornal, J. Jastrzębski, P. Koczoń, J. Kownacki, M. Opacka, T. Pawłat, L. Pieńkowski, W. Płóciennik, J. Sieniawski, P.P. Singh, J. Styczeń, J. Wrzesiński, *Z. Phys.* **A342**, 61 (1992).
[72] A.Y. Abul-Magd, W.A. Friedman, J. Hufner, *Phys. Rev.* **C34**, 113 (1986).
[73] T. von Egidy, H. Daniel, F.J. Hartmann, W. Kanert, E.F. Moser, Ye.S. Golubeva, A.S. Iljinov, J.J. Reidy, *Z. Phys.* **A335**, 451 (1990).
[74] D. Polster, D. Hilscher, H. Rossner, W. Schmid, P. Baumann, H. Daniel, T. von Egidy, F.J. Hartmann, P. Hofmann, Y.S. Kim, M.S. Lotfranei, *Phys. Lett.* **B300**, 317 (1993).
[75] D. Guerreau in "Nuclear Matter and Heavy Ion Collision", M. Soyeur, H. Flocard, B. Tamain and M. Porneuf, Editors, Plenum Publishing Corp., 1989.

[76] J. Galin, U. Jahnke, *J. Phys. G: Nucl. Part. Phys.* **20**, 1105 (1994).
[77] D. Hilscher, W. Bohne, P. Figuera, H. Fuchs, F. Goldenbaum, U. Jahnke, D. Polster, H. Rossner, P. Ziem, J. Galin, B. Lott, M. Morjean, A. Peghaire, B. Quednau, T. von Egidy, F.J. Hartmann, S. Schmid, W. Schmid, K. Gulda, J. Jastrzębski, W. Kurcewicz, L. Pieńkowski, G. Pausch, S. Proschitzki, J. Eades, S. Neumaier, Ye.S. Golubeva, A.S. Iljinov, D.I. Ivanov, V.G. Nedorezov, I.A. Pshenichov, A.S. Sudov *Nucl. Phys.*, in print.
[78] L. Pieńkowski, H.G. Bohlen, J. Cugnon, H. Fuchs, J. Galin, B. Gatty, B. Gebauer, D. Guerreau, D. Hilscher, D. Jacquet, U. Jahnke, M. Josset, X. Ledoux, S. Leray, B. Lott, M. Morjean, A. Peghaire, G. Roschert, H. Rossner, R.H. Siemssen, C. Stephan, *Phys. Rev.* **B336**, 147 (1994).
[79] J. Rafelski, *Phys. Lett.* **B91**, 281 (1980).
[80] J. Rafelski, *Phys. Lett.* **B207**, 371 (1988).
[81] S.B. Kaufman, M.W. Weisfield, E.P. Steinberg, B.D. Wilkins, D. Henderson, *Phys. Rev.* **C14**, 1121 (1976).
[82] W. Gawlikowicz, K. Grotowski, *Nucl. Phys.* **A551**, 73 (1993).